Neglecting acclimation of photosynthesis under drought can cause significant errors in predicting leaf photosynthesis in wheat

Liang Fang, Pierre Martre, Kaining Jin, Xinmiao Du, Peter E L van der Putten, Xinyou Yin, Paul C Struik

RESEARCH ARTICLE

Global Change Biology **WILEY**

Neglecting acclimation of photosynthesis under drought can cause significant errors in predicting leaf photosynthesis in wheat

Liang Fang[1] | Pierre Martre[2] | Kaining Jin[1] | Xinmiao Du[1] |
Peter E. L. van der Putten[1] | Xinyou Yin[1] | Paul C. Struik[1]

[1]Department of Plant Sciences, Centre for Crop Systems Analysis, Wageningen University and Research, Wageningen, The Netherlands

[2]LEPSE, Univ Montpellier, INRAE, Institut Agro Montpellier, Montpellier, France

Correspondence

Xinyou Yin, Department of Plant Sciences, Centre for Crop Systems Analysis, Wageningen University and Research, P.O. Box 430, 6700 AK Wageningen, The Netherlands.
Email: xinyou.yin@wur.nl

Abstract

Extreme climatic events, such as heat waves, cold snaps and drought spells, related to global climate change, have become more frequent and intense in recent years. Acclimation of plant physiological processes to changes in environmental conditions is a key component of plant adaptation to climate change. We assessed the temperature response of leaf photosynthetic parameters in wheat grown under contrasting water regimes and growth temperatures (T_{growth}). Two independent experiments were conducted under controlled conditions. In Experiment 1, two wheat genotypes were subjected to well-watered or drought-stressed treatments; in Experiment 2, the two water regimes combined with high, medium and low T_{growth} were imposed on one genotype. Parameters of a biochemical C_3-photosynthesis model were estimated at six leaf temperatures for each factor combination. Photosynthesis acclimated more to drought than to T_{growth}. Drought affected photosynthesis by lowering its optimum temperature (T_{opt}) and the values at T_{opt} of light-saturated net photosynthesis, stomatal conductance, mesophyll conductance, the maximum rate of electron transport (J_{max}) and the maximum rate of carboxylation by Rubisco (V_{cmax}). T_{opt} for V_{cmax} was up to 40°C under well-watered conditions but 24–34°C under drought. The decrease in photosynthesis under drought varied among T_{growth} but was similar between genotypes. The temperature response of photosynthetic quantum yield under drought was partly attributed to photorespiration but more to alternative electron transport. All these changes in biochemical parameters could not be fully explained by the changed leaf nitrogen content. Further model analysis showed that both diffusional and biochemical parameters of photosynthesis and their thermal sensitivity acclimate little to T_{growth}, but acclimate considerably to drought and the combination of drought and T_{growth}. The commonly used modelling approaches, which typically consider the response of diffusional parameters, but ignore acclimation responses of biochemical parameters to drought and T_{growth}, strongly overestimate leaf photosynthesis under variable temperature and drought.

1 | INTRODUCTION

Extreme climatic events, such as heat waves and drought spells, related to global climate change have become more frequent and intense in recent years (IPCC, 2021; Lloret et al., 2012; Perkins-Kirkpatrick & Lewis, 2020; Solomon et al., 2009). Numerous studies have documented that the impacts of these extreme events are hard to quantify, leading to uncertainties in predicting future gross primary productivity (GPP) and carbon budgets of (agro) ecosystems as well as in assessment of future global food security (Asseng et al., 2015; Lobell & Gourdji, 2012; Peng et al., 2020; Piao et al., 2013; Yin & Struik, 2017). Photosynthesis is the major physiological process that determines GPP of ecosystems and productivity of crops. Scaling up photosynthesis from leaf to canopy and eventually to the GPP of (agro)ecosystems over the whole season requires the quantitative information on how photosynthesis responds to short-term fluctuations, and acclimates to prolonged changes, in environmental variables including extreme events.

The biochemical photosynthesis model of Farquhar, von Caemmerer, and Berry (1980; 'the FvCB model' hereafter) is widely used in quantifying leaf net photosynthesis (A) in response to short-term environmental cues. This model has parameters characterizing various photosynthetic biochemical components, that is, the maximum rate of electron transport (J_{max}) or the maximum rate of carboxylation by Rubisco (V_{cmax}). An extension by Sharkey (1985) adds a third biochemical limitation, the rate of triose phosphate utilization (T_p). This model requires the CO_2 partial pressure at the carboxylation sites (C_c) as input. Thus, conductance for the CO_2 diffusion towards the substomatal cavity (stomatal conductance, g_s) and from the intercellular airspace in leaves to the sites of carboxylation in chloroplasts (mesophyll conductance, g_m) can be coupled with the FvCB model, allowing A to be predicted as a function of the CO_2 level in the intercellular airspaces (C_i) or in the atmospheric air (C_a). Leaf photosynthesis is sensitive to short-term fluctuations in leaf temperature (T_{leaf}): typically, A increases with increasing T_{leaf} up to an optimum temperature (T_{opt}), beyond which A declines with further increases in T_{leaf} (Way & Yamori, 2014; Yamori et al., 2014). This response can be well modelled via temperature responses of photosynthesis parameters (J_{max}, V_{cmax}, T_p, g_s and g_m), typically described using activation energy in the Arrhenius equation (Bernacchi et al., 2009; Rogers et al., 2020).

When plants are exposed to prolonged changes in growth environment [e.g. changes in growth temperatures (T_{growth}) and water regimes], the photosynthetic parameters and their underlying structural, physiological and biochemical processes adjust to these conditions, thereby leading to photosynthetic acclimation (Smith & Dukes, 2013). How leaf photosynthesis adjusts to prolonged changes in T_{growth} and how such adjustments are manifested as

alterations in the response function of a photosynthetic parameter have long been investigated across species (Dusenge et al., 2021; Yamasaki et al., 2002; Yamori et al., 2005). Previous studies reported that while little effect of T_{growth} on V_{cmax} and J_{max} at standard T_{leaf} (25°C; J_{max25} and V_{cmax25}) was observed, photosynthetic acclimation to lower T_{growth} typically results in general downward shifts in T_{opt} of light-saturated net photosynthesis (A_{sat}), J_{max} and V_{cmax} (Kattge & Knorr, 2007; Kumarathunge et al., 2019), as well as in the activation energies of J_{max} (E_{Jmax}) and of V_{cmax} (E_{Vcmax}) (Dusenge et al., 2020; Yin et al., 2019). Likewise, acclimation to higher T_{growth} typically leads to upward shifts in T_{opt} of these parameters. Similar to those for photosynthetic acclimation to elevated CO_2 (Harley et al., 1992; Yin, 2013), mechanisms underlying the acclimation to T_{growth} are possibly linked to leaf N status, as evidence showed that high T_{growth} decreased leaf N, thereby declining photosynthesis capacity (Cai et al., 2020; Crous et al., 2018; Yin et al., 2019). Besides, changes in pigment content and thylakoid membrane may play roles in the acclimation to T_{growth} (Dusenge et al., 2020; von Caemmerer et al., 2009).

Soil water availability also influences leaf photosynthesis. Under drought stress, the decreased photosynthesis could be attributed to lower CO_2 availability induced by stomatal closure (Wei et al., 2020). Kumarathunge et al. (2020) reported that although g_s was significantly lower under water shortage conditions, V_{cmax25} was unaffected, in line with the report of Galmés et al. (2013) of little changes in any of the Rubisco-related parameters under mild to moderate drought. However, photosynthesis under severe water stress can be inhibited by nonstomatal limitations. For instance, drought may induce the occurrence of alternative electron transport (Zivcak et al., 2013), which decreases the proportion of linear electron transport and thus photosynthesis (Yin et al., 2016). Drought stress also impaired ATP synthesis and thus ATP-limited regeneration of RuBP, which in turn decreased Rubisco activity leading to photoinhibition (Flexas & Medrano, 2002). A recent study for wheat showed that drought stress alone did not lead to a decline in Rubisco activation state, whereas the combination of drought and high temperature stress did (Perdomo et al., 2017). Salvucci and Crafts-Brandner (2004) suggested a predominant Rubisco limitation with increasing temperature since high temperature decreases Rubisco's affinity to CO_2 relative to O_2, leading to high photorespiration.

Only accounting for short-term temperature response may not suffice as omitting photosynthetic acclimation to growth environments may overestimate carbon exchange and thus productivity (Smith et al., 2016). There have been many studies on the acclimation responses of photosynthetic parameters to T_{growth} (e.g. Dusenge et al., 2021; Yamasaki et al., 2002), and thermal acclimation parameterizations were developed and have been incorporated in Earth system models (Huang et al., 2019; Kattge & Knorr, 2007; Kumarathunge et al., 2019; Mercado et al., 2018; Smith et al., 2016);

however, this was rarely done for photosynthetic acclimation to other factors and their combination with T_{growth}, probably due to the lack of experimental data. Indeed, recent studies have explored photosynthetic acclimation to more complex environmental combinations, for example, the combination of atmospheric CO_2 and T_{growth} (Cai et al., 2018, 2020; Dusenge et al., 2020) and the combination of ozone and T_{growth} (Dai et al., 2021). Nevertheless, little is known for how photosynthetic components acclimate to water stress and its combination with T_{growth}, which is reflected in the assumptions made in many models that water stress only affects photosynthesis by suppressing g_s but not biochemical parameters (e.g. Yin & Struik, 2017). Kumarathunge et al. (2020) reported that the temperature optima for photosynthesis became lower under water limiting conditions in seedlings of a tree species (*E. tereticornis* sp. *Tereticornis*); however, as the temperature response of biochemical parameters was not reported in their study, they concluded that the photosynthetic acclimation to water stress is mainly attributed to stomatal limitation.

To our knowledge, to date, no single study provides data for full set of leaf photosynthetic parameters and their sensitivity to T_{leaf} in response to a combination of contrasting water regimes and T_{growth}, for a C_3 herbaceous species like wheat. In addition, the consequence of omitting photosynthetic biochemical acclimation to water deficit and T_{growth} in modelling studies remains to be investigated. The objectives of this study are (i) to quantify the response of leaf photosynthetic parameters to T_{growth} and drought; and (ii) to examine to what extent photosynthetic acclimation can affect the results of the FvCB leaf photosynthesis model under severe water deficit at different T_{growth}. We hypothesize that (i) wheat has the ability to adjust its leaf photosynthetic traits to its growing environment, resulting in photosynthetic acclimation in response to drought and that the acclimation to drought depends on T_{growth}; (ii) omitting photosynthetic acclimation to drought and its interactions with T_{growth} in crop growth and plant vegetation models may cause significant errors in predicting leaf photosynthesis and crop yield under climate change scenarios. We conducted experiments in controlled conditions to test the above hypotheses within the context of future warmer and drier climates.

2 | MATERIALS AND METHODS

To test the hypotheses above, we conducted two experiments at Unifarm of Wageningen University, the Netherlands, in 2019 and 2020. In Experiment 1 (EXP2019), two winter wheat (*Triticum aestivum* L.) genotypes, Thésée and Récital, were subjected to well-watered (WW) and drought-stressed (DS) treatments, to determine whether the effect of drought on leaf photosynthesis is genotype dependent; in Experiment 2 (EXP2020), the two water regimes combined with high, medium and low T_{growth} were imposed on Thésée, to examine whether leaf photosynthesis and its components can be altered by contrasting water and T_{growth} regimes. The temperature responses of leaf photosynthesis and its components for each factor combination were examined by estimating parameters of the FvCB model at six T_{leaf}, basically following the procedure of Yin et al. (2009). Temperature response curves were described either by a modified Arrhenius equation (Medlyn et al., 2002) or by a normal distribution alike equation (June et al., 2004). We further quantified the errors created by neglecting the acclimation of both biochemical and CO_2-diffusion parameters. All symbols of model parameters are listed in the Table S1.

2.1 | Experimental set-up and treatments

Plant management practices, experimental set-up and treatments have been detailed in our earlier study (Fang et al., 2022), therefore, only a brief description is given here.

EXP2019 was implemented in a climate-controlled glasshouse. The two genotypes were chosen because of their clear differences in drought tolerance, and precocity, and yield components. Récital was obtained from a cross between a CIMMYT spring wheat cultivar and a French winter wheat breeding line and has higher drought tolerance than Thésée, which was obtained from a cross between a UK feed wheat cultivar and a French bread wheat cultivar. Compared with Récital, Thésée has a stronger cold requirement, a lower tillering capacity and larger grains. Plants were well-irrigated before anthesis. At anthesis half of the plants of each genotype were subjected to a DS treatment by withholding water until the fraction of plant available water declined to ~0.2 (Figure S1c,d; measured by weighing pots daily). At this moment leaf transpiration rate of DS plants was on average ~20% of that of WW plants (Figure S2b); this drought level was maintained by adding to each pot the amount of water lost every day until the end of the measurements (Figure S1). The remaining half of the plants were maintained at 90% soil water holding capacity until the end of the experiment (treatment named WW) as control.

EXP2020 was conducted in climate chambers. When the flag leaf ligule was just visible, which corresponds to the stage of male meiosis (Barber et al., 2015), T_{growth} treatment was applied by allocating plants to three climate chambers with three different day/night air temperature settings: high (28/24°C, daily average temperature 26.7°C; treatment HT), medium (21/17°C, daily average temperature 19.7°C; treatment MT) and low (16/12°C, daily average temperature 14.7°C; treatment LT) temperatures. The T_{growth} settings were similar to the temperature regimes under semi-controlled field conditions as described in Martre et al. (2003). MT is considered as the control growth temperature treatment since the T_{growth} was similar to the outside field temperature (mean temperature 19.5°C) in Martre et al. (2003) and was the same as the T_{growth} before the temperature treatment started. To minimize any confounding impact of varying vapor pressure deficit (VPD), VPD was set identically across chambers (0.87/0.68 kPa for day/night); as a result, 77%, 65% and 52% relative humidity were applied for HT, MT and LT treatments respectively. After anthesis, plants from each chamber were subjected to the two water treatments as in EXP2019.

In both experiments, measurements were labour-intensive and to spread the workload over longer periods of time, four batches of seeds were sown with 10- to 20-day intervals (since crop duration decreases as T_{growth} is increased, and the length of intervals depended on T_{growth} in EXP2020). Within each batch, we established three to five pots of plants for each treatment and the position of pots was rotated daily to avoid any confounding effect of microclimate in the glasshouse or climate chambers.

2.2 | Gas exchange and chlorophyll fluorescence measurements

Gas exchange (GE) and chlorophyll fluorescence (CF) were measured simultaneously on flag leaves by using a portable photosynthetic system (Li-Cor 6800; Li-Cor, Inc.) equipped with an integrated fluorescence chamber head of 6 cm^2. In both experiments, measurements were taken between 10 and 17 days after the onset of the drought treatment, that is, between 147 and 250°C days for LT and between 267 and 454°C days for HT (base temperature 0°C) after anthesis, which broadly corresponds to the start of effective grain filling period (Girousse et al., 2021). Measurements were taken at six T_{leaf} ranging from 15 to 40°C with 5°C intervals, except for the LT treatments in EXP2020 for which T_{leaf} ranged from 12 to 35°C. Leaf-to-air vapor pressure deficit (VPD$_L$) in the cuvette increased when T_{leaf} increased and was controlled at each T_{leaf} step, ranging from 0.9 kPa at 12°C to 3.0 kPa at 40°C (Figure S2a). To achieve the desired T_{leaf}, plants were moved to a climate cabinet with similar air temperatures during measurements.

At each T_{leaf}, light and CO$_2$ response curves (A–I_{inc} and A–C_i curves respectively) were assessed under photorespiratory conditions (PR, 21% O$_2$). For each A–I_{inc} curve, I_{inc} (incident irradiance) was sequentially set at 2000, 1500, 1000, 500, 200, 150, 120, 90, 60 and 40 μmol photons m^{-2} s^{-1} (300–360 s per step), while keeping CO$_2$ concentration in the measurement cuvette (C_a) at 400 ppm. For each A–C_i curve, C_a steps were 400, 200, 100, 50, 400, 400, 400, 650, 1000 and 1500 ppm (150–180 s per step), while keeping I_{inc} at 1000 μmol photons m^{-2} s^{-1}. Prior to each measurement, leaves were first placed in the cuvette with the setting conditions until GE was stable, which took about 30 min. To properly estimate photosynthetic parameters, we also assessed A–I_{inc} curves under non-photorespiratory conditions (NPR, 2% O$_2$ combined with 1000 ppm C_a). To guarantee that data used for calibration were collected within the electron transport-limited range, only the first half of A–I_{inc} curves was measured: I_{inc} was sequentially set at 200, 150, 120, 90, 60 and 40 μmol photons m^{-2} s^{-1} (300–360 s per step), while keeping C_a at 1000 ppm. For the measurements under NPR conditions, a gas cylinder containing a mixture of 2% O$_2$ and 98% N$_2$ was used. Gas from the cylinder was supplied to the Li-Cor 6800 where CO$_2$ was blended with the gas. For each light or CO$_2$ step during GE measurements, the operating photochemical efficiency of photosystem II (Φ_2) was determined at each

I_{inc} or C_a step as $(1 - F_s / F'_m)$ (Genty et al., 1989), where F_s is the steady-state fluorescence, and F'_m is the maximum fluorescence during the saturating light pulse determined by the multi-phase flash method (Loriaux et al., 2013). The three types of curves described above (i.e. the full set of measurements) were assessed on the same flag leaf, and the full set of measurements at each T_{leaf} was conducted randomly during measurement period to minimize any confounding effect of leaf senescence. However, we found it difficult to conduct the full set of measurements on the same flag leaf across all T_{leaf}, as the leaves would be damaged after frequent measurements, especially for drought treatment. Therefore, we used a new leaf when we observed visible damage.

After measurement, the portion of the flag leaves used for GE and CF measurements was cut to determine its N concentration. Rectangle area of the leaf portion was calculated as length multiplied by width which were measured by using a vernier calliper. Then the leaf material was weighed after drying in an oven at 70°C to a constant weight. The concentration of total N in leaf material on a mass basis (N_{mass}, mg g^{-1}) was analysed using an EA1108 CHN-O Element Analyzer (Fisons Instruments) based on the micro-Dumas combustion method. From these data, leaf N content on area basis (N_{area}, g m^{-2}) and leaf mass per area (LMA, g m^{-2}) were calculated.

The GE and CF data of A–I_{inc} curves with I_{inc} ranged from 200 to 40 μmol m^{-2} s^{-1} under PR and NPR conditions of both experiments have previously been used to estimate leaf day respiration (Fang et al., 2022).

2.3 | Estimation of photosynthetic parameters

Values of day respiration (R_d) were taken from our previous estimates for the same experiments (Fang et al., 2022). Photosynthetic parameters of the FvCB model were estimated by using the data of A–I_{inc} and A–C_i curves at each T_{leaf}, following the procedure described by Yin et al. (2009). The full procedure and relevant equations have been detailed in Supplementary Methods of Supporting Information. The estimated parameters included: (i) PSII electron transport efficiency under limiting light (Φ_{2LL}), and the related parameter for the efficiency of converting incident light into linear electron transport under limiting light (κ_{2LL}); (ii) J_{max}; (iii) V_{cmax}; (iv) T_p; (v) g_m. As with previous studies (e.g. Flexas et al., 2007; Ma et al., 2021; Yin et al., 2009), g_m was found to be variable with light and C_i levels, resembling g_s. Here we only report its values for $I_{inc} = 2000$ μmol m^{-2} s^{-1} and $C_a = 400$ ppm (g_{mmax}), together with values of g_s at the same condition for showing A_{sat}. Given that g_{mmax} is a single-point value, we also estimated g_m by the so-called NRH-A method ($g_{m(NRH-A)}$), where g_m is assumed to be constant (Yin & Struik, 2009), by fitting the non-rectangular hyperbolic equation for A to a set of data points of light and CO$_2$ response curves that are expected to be within the electron transport-limited range. Additionally, we calculated the quantum yield of photosynthetic CO$_2$ uptake on an absorbed light basis (Φ_{CO2LL}) under both PR and NPR conditions, according to the procedure of Yin et al. (2014).

2.4 | Temperature responses of photosynthetic parameters

The temperature responses of A_{sat}, g_m, J_{max} and V_{cmax}, wherever possible, were described by a modified Arrhenius equation (Medlyn et al., 2002):

$$X = X_{25}\exp\left[\frac{E_X}{R}\left(\frac{1}{298} - \frac{1}{T_{leaf}}\right)\right]\frac{1 + \exp\left[\frac{D_X}{R}\left(\frac{S_X}{D_X} - \frac{1}{298}\right)\right]}{1 + \exp\left[\frac{D_X}{R}\left(\frac{S_X}{D_X} - \frac{1}{T_{leaf}}\right)\right]} \quad (1)$$

where R is the universal gas constant ($0.008314\,kJ\,K^{-1}\,mol^{-1}$), X_{25} is the value of parameters estimated at $T_{leaf} = 25°C$, E_X, D_X and S_X are the activation energy, deactivation energy and the entropy factor of relevant parameters respectively. To estimate T_{opt} and the value of relevant parameter at T_{opt} (X_{opt}), the same data were fitted to the modified Arrhenius equation written in the form containing T_{opt} (Medlyn et al., 2002; Yin, 2021):

$$X = X_{opt}\frac{D_X\exp\left[\frac{E_X}{R}\left(\frac{1}{T_{opt}} - \frac{1}{T_{leaf}}\right)\right]}{D_X - E_X\left\{1 - \exp\left[\frac{D_X}{R}\left(\frac{1}{T_{opt}} - \frac{1}{T_{leaf}}\right)\right]\right\}} \quad (2)$$

Note that (i) E_X and D_X are common to Equations (1) and (2), and the estimates of E_X or D_X from the two equations are identical (Yin, 2021), and (ii) T_{leaf} in both equations should be in K.

We described the temperature response of Φ_{2LL} and κ_{2LL} by using a normal distribution alike equation (June et al., 2004):

$$X = X_{opt}\exp\left[-\left(\frac{T_{leaf} - T_{opt}}{\Omega}\right)^2\right] \quad (3)$$

where Ω is the value of $T_{leaf} - T_{opt}$ at which Φ_{2LL} or κ_{2LL} falls to $1/e$ (where e is Euler's number) of its value at T_{opt}.

2.5 | Prediction of leaf photosynthetic rate with and without parameter acclimation

We combined the FvCB model [Equations (S1), (S4), (S5), and (S15)] with Equations (1) and (3) to predict A for the different temperature and water regime treatments of both experiments with the estimated photosynthetic parameters and their temperature response curve parameters. To test to what extent omitting photosynthetic acclimation to drought and T_{growth} can affect model predictability, we compared two sets of predictions of A. One was predictions only considering the effect of drought stress or T_{growth} on CO_2 diffusional conductance [g_s and δ_m - a unitless parameter allowing for the variable g_m; see Equation (S14)]. Here the biochemical parameters (κ_{2LL}, J_{max}, V_{cmax}, T_p and R_d) were estimated from plants grown under optimal growth conditions (i.e. treatments WW and MT). This parametrization of the FvCB model is in line with the common practice where only the diffusional limitation is accounted for in modelling the effect of environment variables

on A, namely assuming no biochemical acclimation ('no acclimation') as in an existing crop model (Yin & Struik, 2017). In the second set of predictions, we assumed a 'full acclimation' to growth environmental variables of all photosynthesis biochemical parameters. Thus, in this second set of prediction, we used treatment-specific values of both CO_2 diffusional conductance and biochemical parameters.

We then assessed to what extent each photosynthetic component can independently cause errors in predicting A under variable water supply and T_{growth}. The set of 'full acclimation' was used as a reference to compare errors in A prediction by changing one parameter at a time from their values estimated under treatment-specific conditions (i.e. values of the set of 'full acclimation') to their values estimated under the control growth conditions. Because the shape of temperature response curves is determined together by the shape parameters [e.g. E_X, D_X and S_X in Equation (1)], these parameters were changed together, otherwise the curve would have become biologically meaningless. Therefore, for each photosynthetic parameter, the temperature response curve parameters (if they have) were divided into two parts: one is the value of relevant photosynthetic parameters estimated at a reference T_{leaf} [i.e. X_{25} in Equation (1) and X_{opt} in Equation (3)], and the other is the shape parameters of the curve [i.e. E_X, D_X and S_X in Equation (1), Ω and T_{opt} in Equation (3)]. Here, values of the temperature response curve parameters of R_d were taken from Fang et al. (2022), and the temperature response of R_d was described by the simple Arrhenius equation [E_X is the only shape parameter; see equation (6) in Fang et al., 2022].

2.6 | Curve fitting and model analyses

Non-linear curve fitting procedures in the FvCB model, Equations (1)–(3) were implemented using the GAUSS method in PROC NLIN of SAS (SAS Institute, Inc.). The SAS codes can be obtained upon request to the corresponding author. We fitted the GE and CF data by using pooled data of individual replicates to obtained estimates of photosynthetic parameters, which are most reliable for representing treatment-specific parameters (which in fact are close to the mean of replicated estimates but have better statistical predictions of all data points than the mean). Therefore, the parameters of the modified Arrhenius equation [Equations (1) and (2)] and the normal distribution alike equation [Equation (3)] and their standard error of the estimates were estimated by using the parameter estimates estimated from the pooled data.

We assessed the goodness of the predictions of A with and without acclimation of the photosynthesis biochemical parameters using the relative root mean squared error (rRMSE) given by:

$$rRMSE = \frac{1}{\bar{x}}\sqrt{\frac{\sum_{i=1}^{n}(y_i - x_i)^2}{n}} \quad (4)$$

where n is the number of data points, and $\bar{x}$ is the mean of the measured values, y_i and x are the ith predicted and measured values respectively. Model analyses for prediction of A with and without parameter acclimation were conducted using R version 4.1.2 (R Foundation).

3 | RESULTS

The above-mentioned photosynthetic parameters were estimated for each T_{leaf}, based on the GE and CF measurements on the well-watered and severe water-stressed plants grown under various T_{growth}, thereby, their temperature responses were obtained, as described below.

3.1 | Temperature response of light-saturated net photosynthesis

In EXP2019, drought decreased A_{sat} at the optimum temperature ($A_{sat,opt}$) and at 25°C ($A_{sat,25}$), as well as the optimum temperature for A_{sat} ($T_{opt,Asat}$) for both genotypes (Figure 1a; Table S5). In EXP2020, the response of A_{sat} to T_{leaf} was altered by both the water and T_{growth} treatments (Figure 1b; Table S6). For WW plants, $T_{opt,Asat}$ increased with increasing T_{growth}, while $A_{sat,opt}$ was not significantly affected by T_{growth} treatments (Table S6). The drought treatment suppressed A_{sat} at all T_{leaf}, and this drought effect differed among the T_{growth} treatments. For the three T_{growth} treatments, $T_{opt,Asat}$ was 3.5–7°C lower for DS than for WW. Moreover, unlike for WW, for DS $A_{sat,opt}$ differed between T_{growth}, with its value being lowest for HT and highest for MT (Figure 1b; Table S6).

3.2 | Temperature response of CO₂ diffusional conductance

Generally, for WW plants of EXP2019 and those grown at MT in EXP2020, g_s increased with T_{leaf} up to a maximum value at ~25°C and decreased at higher T_{leaf}, but increased again at 40°C (also high VPD_L, Figure 2a,b; Figure S2f), agreeing with results from previous report (Slot et al., 2016). For both genotypes, the optimum

temperature for g_s ($T_{opt,gs}$) was 5°C lower for DS than for WW (Figure 2a). For EXP2020, $T_{opt,gs}$ increased with increasing T_{growth} for both water treatments (Figure 2b). Drought stress suppressed g_s at all T_{leaf} (Figure 2a,b).

Drought stress declined g_{mmax} at its optimum temperature ($g_{mmax,opt}$) and at 25°C ($g_{mmax,25}$) for both genotypes and for all T_{growth} (Tables S5 and S6). In EXP2019, under DS conditions the optimum temperature for g_{mmax} ($T_{opt,gmmax}$) slightly decreased for both genotypes; while in EXP2020, the shift of $T_{opt,gmmax}$ was obvious for LT but not for HT and MT (Figure 2c,d). Similarly, drought stress decreased $g_{m(NRH-A)}$ at all T_{growth} for $T_{leaf} > 20°C$ (Figure 2e,f). The drought treatment decreased the optimum temperature for $g_{m(NRH-A)}$ ($T_{opt,gm(NRH)}$), regardless of genotypes and T_{growth}, and this decrease differed among T_{growth} (Figure 2e,f).

3.3 | Temperature response of electron transport parameters and quantum yield

Φ_{2LL} showed a limited response to T_{leaf}, which is in line with previous results (Bernacchi et al., 2003; Yin et al., 2014). In EXP2019, Φ_{2LL} was roughly consistent between genotypes but slightly lower for DS compared with WW at all T_{leaf} (Figure 3a,c; Table S7). For WW in EXP2020, Φ_{2LL} was not significantly affected by T_{growth}, while drought stress increased the optimum temperature for Φ_{2LL} ($T_{opt,\Phi2LL}$) for all T_{growth} under PR conditions (Figure 3b,d; Table S8).

The calculated κ_{2LL} also showed a bell-shape response to T_{leaf} (Figure 3e,f). In EXP2019, for both genotypes, κ_{2LL} appeared to respond more to T_{leaf} under DS than under WW (Figure 3e). Drought stress decreased κ_{2LL} at all T_{leaf}, accompanied with decreases in the optimum temperature for κ_{2LL} ($T_{opt,\kappa2LL}$) and its value at $T_{opt,\kappa2LL}$ ($\kappa_{2LL,opt}$; Tables S7 and S8). In EXP2020, $\kappa_{2LL,opt}$ decreased with increasing T_{growth} under both water regimes and $T_{opt,\kappa2LL}$ was higher for HT than for MT and LT (Figure 3f; Table S8).

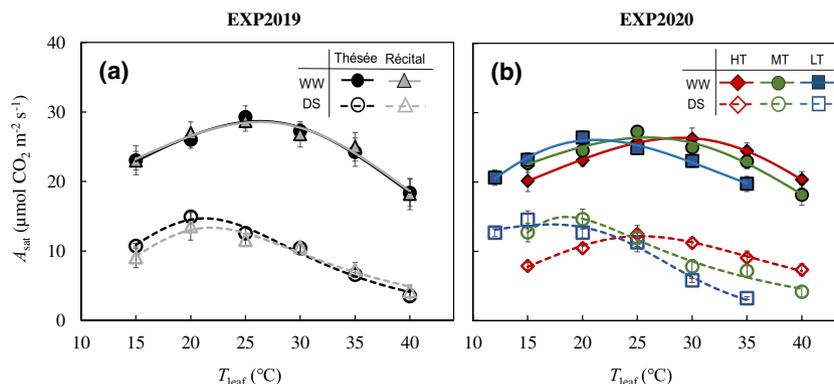**FIGURE 1** Temperature response of light-saturated net CO_2 assimilation rate (A_{sat}). Response of measured A_{sat} to leaf temperatures (T_{leaf}) for the winter wheat genotypes Thésée (circles) and Récital (triangles) grown in a glasshouse under well-watered (WW; filled symbols and solid lines) or drought-stressed (DS; open symbols and dashed lines) conditions in EXP2019 (a), and for Thésée grown in climate chambers at high (HT, day/night temperature 28/24°C; rhombuses), medium (MT, day/night temperature 21/17°C; circles) or low (LT, day/night temperature 16/12°C; rectangles) growth temperature under WW (filled symbols and solid lines) or DS (open symbols and dashed lines) conditions in EXP2020 (b). A_{sat} was measured at an incident irradiance of 2000 μmol m⁻² s⁻¹ and a C_a of 400 ppm. Curves were drawn according to the modified-Arrhenius equation, Equation (1), fitted to the data. Data are means ± 1 SE for n = 4–7 independent replicates.
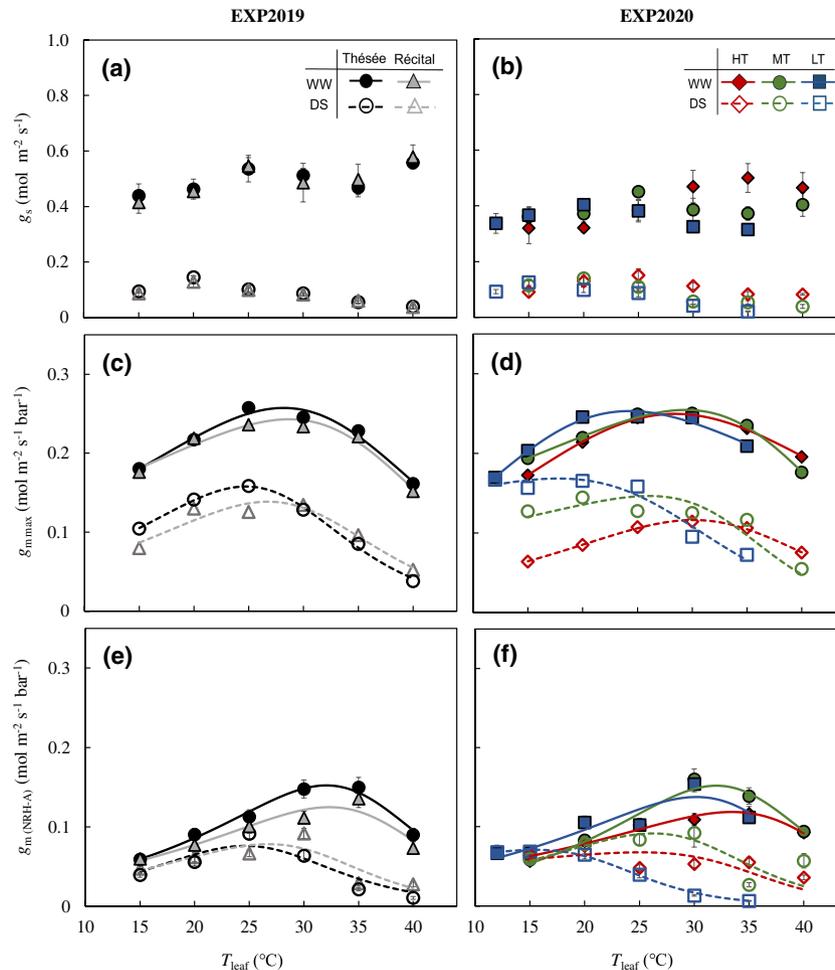
FIGURE 2 Temperature response of CO_2 diffusional conductance. Responses of stomatal conductance measured at an incident irradiance of 2000 μmol m^{-2} s^{-1} and a C_a of 400 ppm [g_s; (a, b)], and mesophyll conductance estimated for the same conditions [g_{mmax}; (c, d)] and by the NRH-A method [$g_{m(NRH-A)}$; (e, f)] to leaf temperature (T_{leaf}) for the winter wheat genotypes Thésée and Récital grown in a glasshouse under well-watered (WW; filled symbols and solid lines) or drought-stressed (DS; open symbols and dashed lines) conditions in EXP2019 (a, c, e), and for Thésée grown in climate chambers at high (HT, day/night temperature 28/24°C; circles), medium (MT, day/night temperature 21/17°C; triangles) or low (LT, day/night temperature 16/12°C; rectangles) growth temperature under WW (filled symbols and solid lines) or DS (open symbols and dashed lines) conditions in EXP2020 (b, d, f). In (c–f) curves were drawn according to the modified-Arrhenius equation, Equation (1), fitted to the data. In (a) and (b) data are means ± 1 SE for n = 4–7 independent replicates, and in (e) and (f) data are estimates ± 1 SE for n = 4–7 independent replicates.

The quantum yield of photosynthetic CO_2 uptake (Φ_{CO2LL}) depended significantly on T_{leaf}, water regime, and photorespiratory condition, but not on genotype or T_{growth} (Figure 4). Under PR conditions, drought stress increased the sensitivity of Φ_{CO2LL} to T_{leaf}. Under NPR conditions, Φ_{CO2LL} of WW plants was essentially independent of T_{leaf} (Figure 4c,d); however, for DS treatment, even under NPR conditions, Φ_{CO2LL} decreased with increasing T_{leaf}, although the temperature sensitivity of Φ_{CO2LL} was weaker than for PR (Figure 4).

3.4 | Temperature response of photosynthetic capacity parameters

For both genotypes, under WW conditions J_{max} increased with increasing T_{leaf} but declined for $T_{leaf} > \sim33°C$ (Figure 5a). J_{max} decreased

under DS conditions at all T_{leaf} and its optimum temperature ($T_{op,Jmax}$) was 8°C lower for DS compared with WW (Figure 5a; Table S5). $T_{opt,Jmax}$ increased with increasing T_{growth} for both WW and DS, and it was ~10°C lower for DS than for WW at each T_{growth} (Figure 5b; Table S6).

In general, V_{cmax} for WW plants increased exponentially with T_{leaf}; drought stress slightly decreased V_{cmax} while this decrease was significant for $T_{leaf} > 25°C$ (Figure 5c,d). The optimum temperature for V_{cmax} ($T_{opt,Vcmax}$) was lower for DS than for WW, but except for the case of HT in EXP2020 (Figure 5c,d). The ratio of J_{max} to V_{cmax} decreased with increasing T_{leaf} irrespective of the water and T_{growth} treatment (Figure S3).

As in previous studies (Harley & Sharkey, 1991; Yang et al., 2016), here the rate of triose phosphate utilization (T_p) increased as T_{leaf} increased from 15 to 30°C. However, T_p was not estimated for
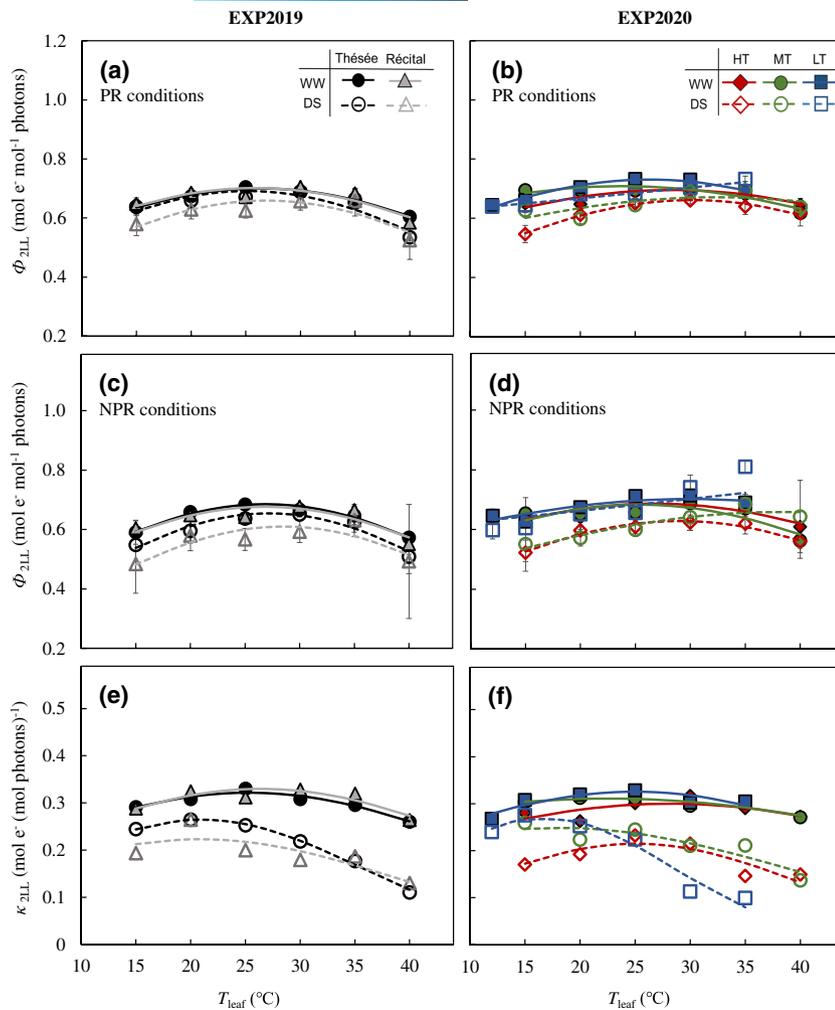
FIGURE 3 Temperature response of electron transport parameters. Responses of quantum efficiency of photosystem II electron transport at limiting light (Φ_{2LL}) for photorespiratory [PR; (a, b)] and non-photorespiratory [NPR; (c, d)] conditions, and calculated conversion efficiency of limiting incident light into linear electron transport of photosystem II [κ_{2LL}; (e, f)] to leaf temperature (T_{leaf}) for the winter wheat genotypes Thésée and Récital grown in a glasshouse under well-watered (WW; filled symbols and solid lines) or drought-stressed (DS; open symbols and dashed lines) conditions in EXP2019 (a, c, e), and for Thésée grown in climate chambers at high (HT, day/night temperature 28/24°C; circles), medium (MT, day/night temperature 21/17°C; triangles) or low (LT, day/night temperature 16/12°C; rectangles) growth temperature under WW (filled symbols and solid lines) or DS (open symbols and dashed lines) conditions in EXP2020 (b, d, f). Curves were drawn according to the modified-Arrhenius equation, Equation (1), fitted to the data. In (a–d) data are estimates ± 1 SE for $n = 4$–7 independent replicates.

$T_{leaf} > 30$°C (in EXP2019) or 35°C (in EXP2020) for WW and for $T_{leaf} > 20$°C (in EXP2019) or 25°C (in EXP2020) for DS (Figure 5e,f), indicating little limitation set by triose phosphate utilization. Therefore, no temperature response curve was drawn for T_p in Figure 5e,f.

3.5 | Effects of neglecting acclimation to growth environments on the prediction of photosynthetic rate

Since we found considerable acclimation of photosynthesis to drought and T_{growth}, we assessed to what extent the results of the FvCB model may be affected by different growth and measurement conditions. A was simulated using the model with and without drought and T_{growth} acclimation of photosynthetic biochemical parameters (κ_{2LL}, J_{max}, V_{cmax}, T_p and R_d). The simulated results were compared with measured A under specific growth conditions. As stated earlier, for both sets of simulations, the acclimation of CO_2 diffusional conductance was considered.

When no acclimation of biochemical parameters was considered, the FvCB model overestimated A under drought stress by 37%–87%, with rRMSE >1 (Figure 6a,c,e,i). The difference between measured and simulated A increased as T_{leaf} increased, especially for plants

grown at MT and LT (Figure 6e,i). In contrast, when the acclimation of photosynthetic biochemical parameters was considered, the FvCB model gave good results for all treatments (Figure 6b,d,f,j). For comparison, omitting CO_2 diffusional conductance acclimation under drought increased error values across genotypes and T_{growth}. In addition to CO_2 diffusional conductance, omitting drought acclimation of electron transport parameters (J_{max} and κ_{2LL}) also led to considerable errors under all T_{growth}, but the error values varied among T_{growth} (Figure 7a). However, when neglecting the drought acclimation of other biochemical parameters (V_{cmax}, R_d and T_p), the errors were insubstantial as compared with neglecting the acclimation of CO_2 diffusional and electron transport parameters (Figure 7a). On the other hand, when neglecting T_{growth} acclimation, the model did not overestimate A, while the difference between measured and simulated A was larger in 'no acclimation' set than in 'full acclimation' set (Figure 6g,k). The larger variability was attributed to V_{cmax} and R_d under HT and to J_{max} and CO_2 diffusional conductance under LT (Figure 7b).

4 | DISCUSSION

Plants have a strong ability to adjust their photosynthetic capacity in response to both short- (seconds to minutes) and long-term (days
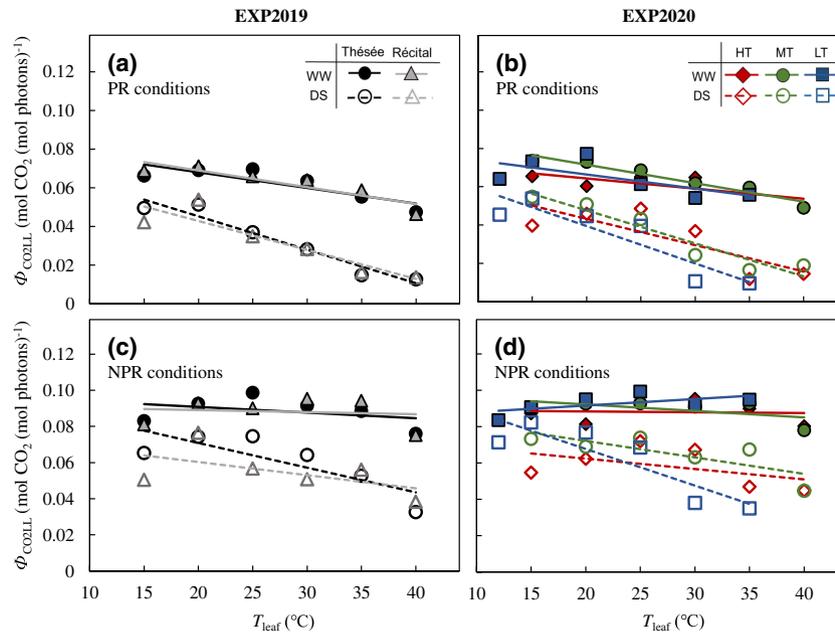
FIGURE 4 Temperature response of quantum yield. Responses of quantum yield of photosynthetic CO_2 uptake (Φ_{CO2LL}) for photorespiratory [PR, (a, b)] and non-photorespiratory [NPR, (c, d)] conditions to leaf temperature (T_{leaf}) for the winter wheat genotypes Thésée and Récital grown in a glasshouse under well-watered (WW; filled symbols and solid lines) or drought-stressed (DS; open symbols and dashed lines) conditions in EXP2019 (a, c), and for Thésée grown in climate chambers at high (HT, day/night temperature 28/24°C; circles), medium (MT, day/night temperature 21/17°C; triangles) or low (LT, day/night temperature 16/12°C; rectangles) growth temperature under WW (filled symbols and solid lines) or DS (open symbols and dashed lines) conditions in EXP2020 (b, d). Lines are linear regressions fitted to the data of each genotype and treatment.

to weeks) changes in environmental conditions (Moore et al., 2021; Posch et al., 2019). In the present study, we investigated if temperature responses of photosynthesis components acclimate to seasonal T_{growth} and long-term severe water deficit and to what extent the acclimation of photosynthetic parameters to environmental variables can affect the predictability of the FvCB model. Main results about the acclimation responses of various photosynthetic parameters are discussed as follows.

4.1 | General photosynthetic acclimation responses to growth temperature and drought

In general, $A_{sat,opt}$ was not affected by T_{growth} under WW conditions, but its temperature response acclimated strongly to both drought and T_{growth}. We found drought stress lowered $T_{opt,Asat}$ across T_{growth}, which was consistent with findings of a recent study in Eucalyptus trees (Kumarathunge et al., 2020), implying that C_3 grasses and C_3 trees may respond similarly to water stress. Moreover, $T_{opt,Asat}$ and T_{opt} of other photosynthetic components (e.g. g_m, κ_{2LL}, J_{max} and V_{cmax}) were more sensitive to T_{growth} under DS conditions (Figure S4), and were closer to daytime T_{growth} under DS than under WW conditions, implying that the adverse conditions forced plants to acclimate more in order to maximize CO_2 uptake for survival. Our previous study showed that there is an interactive effect of drought and T_{growth} on the sensitivity of R_d to T_{leaf} (Fang et al., 2022), and consequently the $R_d/(A_{sat}+R_d)$ ratio was altered by drought and T_{growth}, suggesting that

leaf carbon use efficiency, that is, $[1-R_d/(A_{sat}+R_d)]$, was altered by environmental changes (Figure S5).

Previous studies suggested that photosynthetic acclimation to long-term changes in environmental variables (e.g. CO_2 elevation and/or T_{growth} elevation) is mainly due to the changes in leaf nitrogen status, as they found linear relationships between photosynthetic parameters and leaf nitrogen content across various environmental factors (Cai et al., 2020; Harley et al., 1992; Yin, 2013). However, we found that photosynthetic parameters generally showed poor correlations with N_{area} across T_{growth} and water regimes despite weak correlations within the drought treatment (Figure S6a–d). Part of the reasons for the poor correlation is that our values of N_{area} was only in the narrow, high range of leaf N (i.e. from 1.5 to 2.5 g N m^{-2}, agreeing with previously recorded ~2 g N m^{-2} for wheat with sufficient N supply; Cai et al., 2020; Wang et al., 2022; Yin et al., 2019). Along with the acclimation of the above physiological and biochemical processes, we found that the leaf morphological trait LMA also acclimated to environmental variables. Again, little correlation was observed between photosynthetic parameters and LMA (Figure S6e–h).

4.2 | Acclimation responses in CO_2 diffusional conductance to growth temperature and drought

A previous study observed that the shape of the response of g_s to T_{leaf} is not modified by T_{growth}, although g_s is higher under high T_{growth} than under low T_{growth} (Yamori et al., 2006). However, our results
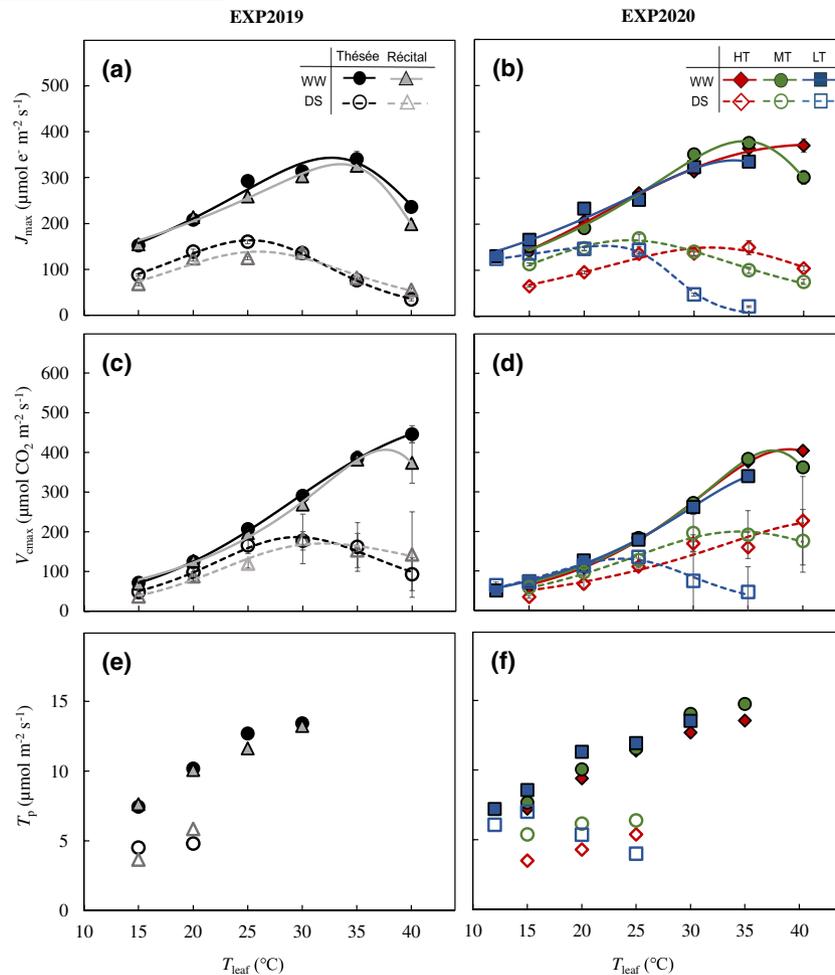
FIGURE 5 Temperature response of photosynthetic capacity parameters. Responses of the maximum rate of electron transport [J_{max}; (a, b)], the maximum rate of carboxylation by rubisco [V_{cmax}; (c, d)], and triose phosphate utilization [T_p; (e, f)] to leaf temperature (T_{leaf}) for the winter wheat genotypes Thésée and Récital grown in a glasshouse under well-watered (WW; filled symbols and solid lines) or drought-stressed (DS; open symbols and dashed lines) conditions in EXP2019 (a, c, e), and for Thésée grown in climate chambers at high (HT, day/night temperature 28/24°C; circles), medium (MT, day/night temperature 21/17°C; triangles) or low (LT, day/night temperature 16/12°C; rectangles) growth temperature under WW (filled symbols and solid lines) or DS (open symbols and dashed lines) conditions in EXP2020 (b, d, f). J_{max} and V_{cmax} at T_{leaf} of 35 and 40°C for DS plants grown at HT and MT were estimated by fitting across-replication average values due to the large variation of data under combined drought and high T_{leaf} conditions. In (a–d), data are estimates ± 1 SE for $n = 4–7$ independent replicates, and curves were drawn according to the modified-Arrhenius equation, Equation (1), fitted to the data.

showed that T_{growth} altered not only the magnitude of g_s values but also the shape of the response of g_s to T_{leaf}. For WW plants in EXP2019 and those grown at MT in EXP2020, g_s increased again when T_{leaf} was >35°C, whereby leaf cooling increased. This is consistent with recent studies suggesting that there could be a decoupling between A and g_s resulting in a trade-off between carbon gain and evaporative cooling at extremely high temperature when water availability is unlimited (Moore et al., 2021; Slot et al., 2016).

The shape of the response of either g_{mmax} or $g_{m(NRH-A)}$ to T_{leaf} under WW conditions was similar to that previously reported (Warren, 2008 and references therein). Drought stress altered the shape of the response of g_{mmax} to T_{leaf} for both genotypes for all T_{growth} by decreasing $T_{opt,gmmax}$ and/or $g_{mmax,opt}$. Moreover, T_{growth} altered $T_{opt,gm(NRH-A)}$ and $g_{m(NRH-A),opt}$ under both WW and DS conditions, while this alteration was only obvious under DS conditions

for g_{mmax}. These alterations by water stress and T_{growth} suggest that g_m could acclimate to environmental variables and this acclimation could be associated with changes in physical and anatomical properties (e.g. cell wall thickness, surface area of chloroplasts) and in proteins and enzymes, for example, aquaporins and carbonic anhydrase (Flexas & Diaz-Espejo, 2015; Ouyang et al., 2017; von Caemmerer & Evans, 2015).

4.3 | Acclimation responses of electron transport and quantum yield to growth temperature and drought

Previous studies indicated that the thermal response curve of Φ_{2LL} is parabolic (Yin et al., 2014) and its shape is unaffected by T_{growth}
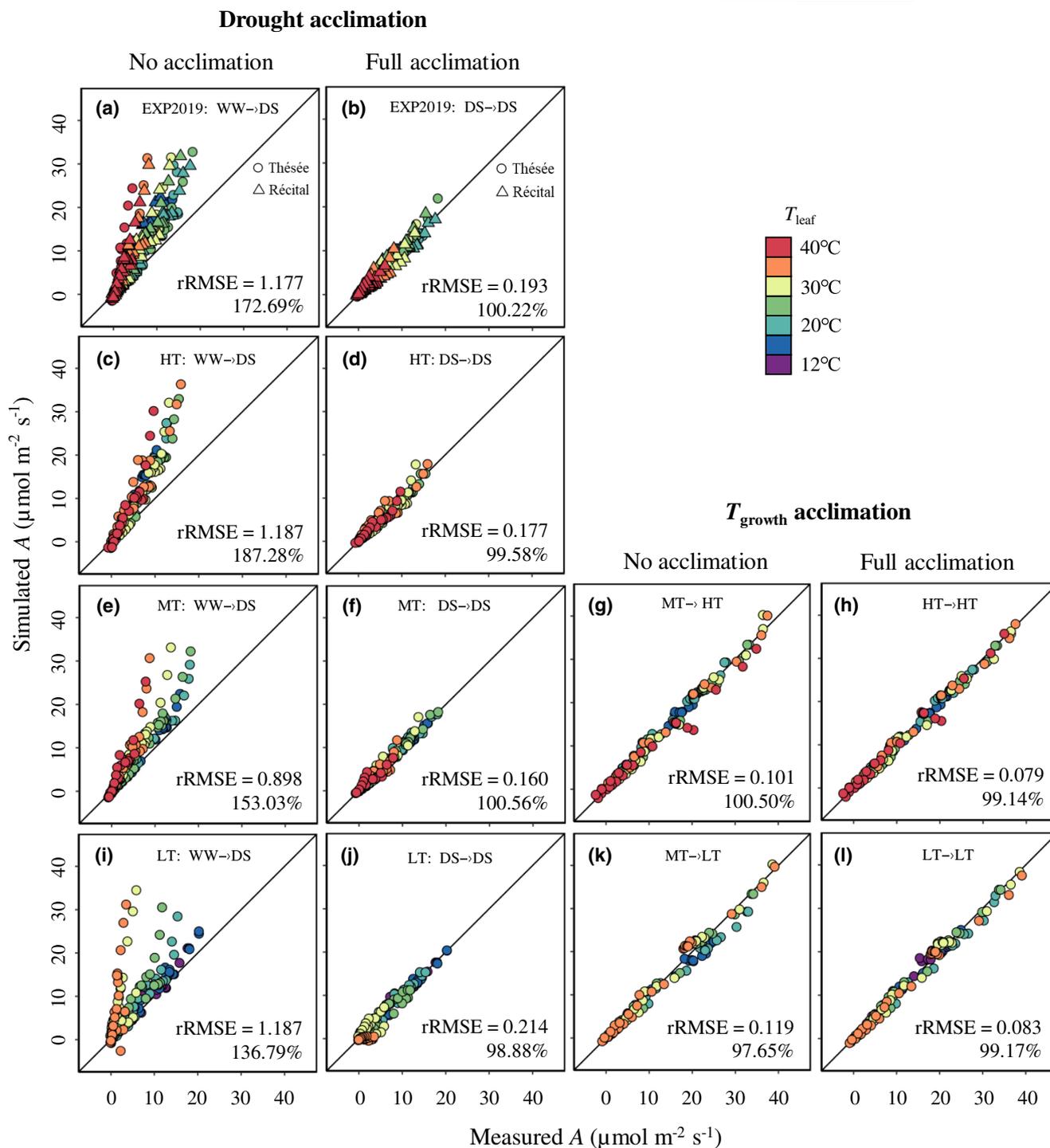
FIGURE 6 Comparisons between measured and simulated net CO_2 assimilation rate (A). Comparisons between measured A and simulated A either considering only the acclimation of CO_2 diffusional parameters but omitting the acclimation of photosynthetic biochemical parameters (a, c, e, i, g, k, no acclimation) or considering the acclimation of both CO_2 diffusional and photosynthetic biochemical parameters (b, d, f, j, h, l, full acclimation), across treatments and measurement conditions. The text in each panel with an arrow, for example, WW→DS, means using the parameters estimated under the well-watered (WW) treatment as inputs to predict A under the drought-stressed (DS) treatment (other treatment abbreviations: LT, low growth temperature; MT, medium growth temperature; HT, high growth temperature). The solid diagonal represents the 1:1 relationship. The percentage in each panel is the average of simulated relative to observed A. rRMSE is the relative root mean squared error, as defined by Equation (4).

(Bernacchi et al., 2003). Here, our data showed that neither T_{growth} nor the genotype affected T_{leaf} dependency of Φ_{2LL}. However, drought stress slightly decreased Φ_{2LL} at lower T_{leaf}, but not for

$T_{leaf} > 35°C$, leading to increases in $T_{opt,\Phi2LL}$. This is in agreement with an earlier study showing an increased thermostability of PSII to heat stress in drought-stressed plants (Lu & Zhang, 1999).
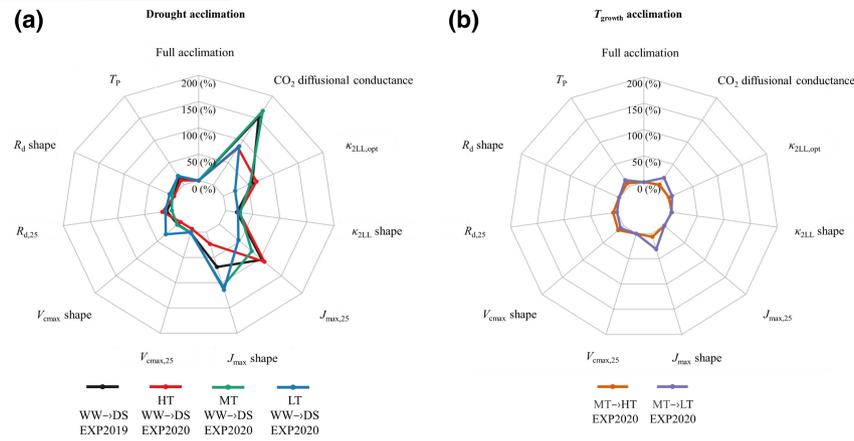
FIGURE 7 Relative changes (%) in relative root mean squared error (rRMSE) of model prediction. Relative changes in rRMSE of model prediction using different sets of parameter values relative to that of prediction assuming the 'full acclimation', for data involving responses to drought (a) or involving responses to growth temperature (b). To what extent photosynthetic parameters can independently cause errors in predicting net CO_2 assimilation was assessed by fixing these parameters, one at a time, from their values estimated under treatment-specific conditions (i.e. values of the set of 'full acclimation') to their values estimated under optimal growth conditions (i.e. parameter values assuming no acclimation to growth conditions). The higher relative change in percentage means a greater error in predictions when their acclimations were neglected. Text in the figure legend with an arrow, for example, WW→DS, means using the parameters estimated under the well-watered (WW) treatment as inputs to predict A under the drought-stressed (DS) treatment (other treatment abbreviations: LT, low growth temperature; MT, medium growth temperature; HT, high growth temperature). Note that parameters of temperature response curve were divided into two parts: One is the parameter value at a reference T_{leaf} [i.e. X_{25} for Equation (1) and X_{opt} for Equation (3)]; the other is the shape parameters of the temperature response curve [i.e. E_X, D_X and S_X for Equation (1), Ω and T_{opt} for Equation (3)].

Yin et al. (2014) suggested that both Φ_{2LL} and the slope factor [$s'_{(abs)}$ and $s_{(abs)}$, see Equation (S19)] should be accounted for to estimate Φ_{CO2LL}. $s_{(abs)}$ lumps two parameters: the interphotosystem energy partitioning (ρ_2), and the alternative electron fraction in the form of $[1 - f_{pseudo} / (1 - f_{cyc})]$. $s'_{(abs)}$ is multiplied by an additional term $[(C_c - \Gamma_*) / (C_c + 2\Gamma_*)]$, see Equation (S19). In line with the results of Yin et al. (2014), our data showed that the response of Φ_{CO2LL} to T_{leaf} was also parabolic, which was attributed to Φ_{2LL}, while the difference in Φ_{CO2LL} response to T_{leaf} between different photorespiratory conditions could be explained by the term $[(C_c - \Gamma_*) / (C_c + 2\Gamma_*)]$ (i.e. the amount of photorespiration). The higher relative loss due to photorespiration [as indicated by $\left(s_{(abs)} - s'_{(abs)}\right) / s_{(abs)}$; Figure S7] in DS plants and the increased photorespiration with increased T_{leaf} could be responsible for the stronger T_{leaf} sensitivity of Φ_{CO2LL} under PR conditions across water regimes and T_{growth}. However, Φ_{CO2LL} under NPR conditions still differed between WW and DS plants, suggesting that photorespiration was not the only reason for the different thermal sensitivity. Our previous study has demonstrated that the gas mixture we used (2% O_2 combined with 1000 ppm C_a) for estimating the calibration factor (i.e. $s_{(abs)}$ here) did allow to reach a nearly NPR state, even for extreme conditions (Fang et al., 2022). Given that ρ_2 most likely does not vary much, the declines in Φ_{CO2LL} with increasing T_{leaf} in DS plants under NPR conditions indicated that the second parameter $[1 - f_{pseudo} / (1 - f_{cyc})]$, see Equation (S19), increased significantly under drought, especially when combined with high temperature. The increase in this parameter, representing the overall fraction for alternative electron transport (Yin et al., 2016), agrees with the result of Zivcak et al. (2013) that alternative electron transport operates as a means of photoprotection under drought.

4.4 | Acclimation responses in photosynthetic capacity parameters to growth temperature and drought

The effects of T_{growth} on photosynthetic capacity parameters (i.e. J_{max} and V_{cmax}) have been widely investigated but with inconsistent results (Kattge & Knorr, 2007; Kumarathunge et al., 2019). As compared with T_{growth}, drought stress exerted a greater impact on photosynthetic capacity. J_{max} was significantly suppressed under DS conditions and the effect of drought on J_{max} increased as T_{leaf} increased. $T_{opt,Jmax}$ was lower under DS conditions compared to WW conditions, although the extent of the decrease in $T_{opt,Jmax}$ under drought depended on T_{growth}. Previous studies have indicated that drought stress can lead to damage of the electron transport chain, along with ATP shortage, thereby limiting the regeneration of RuBP, that is, J_{max} (Campos et al., 2014; Tezara et al., 1999). However, damage to the electron transport chain cannot explain the decreased $T_{opt,Jmax}$ observed here. Changes in $T_{opt,Jmax}$ in response to T_{growth} may be associated with the thermal acclimation of the thylakoid membrane (von Caemmerer et al., 2009). Thus, we speculate that the acclimation of the thylakoid membrane may also occur when plants are grown under drought stress, and it is conceivable that this acclimation to drought would be different under contrasting T_{growth}.

Our results showed that the decrease in V_{cmax} under drought was limited for $T_{leaf} < 25°C$ for both genotypes and for all T_{growth}. This is consistent with Galmés et al. (2013) who reported that the effects of drought on Rubisco-related parameters were not significant or only minor across species and studies, and with Kumarathunge

et al. (2020) who showed that $V_{cmax,25}$ values were similar between two different water regimes across various T_{growth}. Moreover, in vitro assays showed that Rubisco activity and Rubisco carboxylase maximum turnover rate decrease only for measurement temperature >50°C (Galmés et al., 2015; Salvucci & Crafts-Brandner, 2004). Therefore, although a decrease in V_{cmax} has sometimes been observed at extremely high T_{leaf} (Leuning, 2002; Medlyn et al., 2002), the temperature response of V_{cmax} was originally modelled by the simple non-peaked Arrhenius equation (Farquhar et al., 1980). This is supported by our data under well-watered conditions, where $V_{cmax,Topt}$ was mostly not observed up to our highest T_{leaf} of 40°C. However, surprisingly, $T_{opt,Vcmax}$ was decreased by drought, owing to the substantial decrease in V_{cmax} for $T_{leaf} > \sim 30°C$. The decrease in g_m under drought suggested that low C_c under drought stress might cause the decrease in $T_{opt,Vcmax}$. Evidence showed that low C_c could induce the deactivation of Rubisco sites (Galmés et al., 2011). Hikosaka et al. (2006) and Yamori et al. (2014) also indicated that changes in activity and thermal lability of Rubisco and Rubisco activase might also be involved in drought acclimation. Therefore, our observed decline of V_{cmax} at high T_{leaf} under drought might reflect drought induced changes not only in the activity but also in activation state of Rubisco. The full mechanisms behind the complex interactive effect of drought stress and T_{growth} on the response of V_{cmax} to T_{leaf} (Figure 5d) remain to be elucidated.

4.5 | The necessity of considering acclimation of photosynthetic components when projecting photosynthesis under various growth conditions

Projecting future GPP in the context of climate change is strongly affected by uncertainties in not only the short-term but also the long-term responses of photosynthetic parameters to environmental variables. Although photosynthetic acclimation to T_{growth} has been empirically modelled (Huang et al., 2019; Mercado et al., 2018; Smith et al., 2016), uncertainties remain, as this acclimation could be interactively affected by other environmental variables, for instance, the interaction between T_{growth} and drought as shown in our study.

Earlier photosynthesis models only assumed that water stress directly affects photosynthesis through g_s (e.g. Yin & van Laar, 2005). Using Equations (S14) and (S15) would indirectly account for the drought effect on the other diffusional parameter g_m, which has been incorporated into recent crop models (e.g. Yin & Struik, 2017). But overall, these models still do not account for drought acclimation of biochemical parameters. However, our study revealed that although the CO_2 diffusional parameters matter substantially for model prediction, biochemical parameters (κ_{2LL}, J_{max}, V_{cmax}, T_p and R_d) also acclimate to various environments, and consequently our results clearly showed that neglecting this acclimation leads to critical errors in predicting A (Figures 6 and 7). Moreover, simulation analysis showed that omitting drought acclimation of κ_{2LL} and J_{max}, both for values estimated at a reference T_{leaf} and the shape parameters,

resulted in significant errors in predicting leaf photosynthetic rate; while the influence of omitting the acclimation of V_{cmax}, T_p or R_d was limited (Figure 7). These results are in line with the reports of Gu et al. (2014), Yin et al. (2022) and Harbinson and Yin (2022), who showed electron transport parameters, rather than Rubisco-related parameters (i.e. V_{cmax}), contribute most to the variation of plant productivity. Nevertheless, V_{cmax}, T_p and R_d still had influence on the prediction of photosynthetic capacity (Figure 7). Our results suggest that the acclimation of these biochemical parameters to environmental variables should not be neglected as well, in particular under drought conditions and at high T_{leaf}.

Kattge and Knorr (2007) proposed simple algorithms to represent and parameterize the temperature acclimation of biochemical parameters of photosynthesis across 36 C_3 species, thereby allowing the acclimation to be implemented directly in models. The algorithms were later extended by Kumarathunge et al. (2019) with broader ranges of species and geographical gradients. However, none of these previous studies addressed acclimation parameterization of photosynthetic components under water stress. Although we provided a clear case to demonstrate the necessity to consider drought acclimation of biochemical parameters in predicting photosynthesis, more experimental work and theoretical analysis on how biochemical parameters acclimate to water stress under various T_{growth} and levels of water deficit, for different species and geographical locations is urgently needed.

4.6 | Concluding remarks

Typical practices in ecophysiological and modelling studies on the impact of climate change variables on (agro)ecosystems assume: (i) photosynthetic acclimation to environmental factors (e.g. elevated CO_2 and/or elevated T_{growth}) is associated with altered leaf N content (e.g. Cai et al., 2020; Dusenge et al., 2020; Yin, 2013), and (ii) the impact of water stress on photosynthesis is via the decrease in diffusional parameters (e.g. Centritto et al., 2009; Kumarathunge et al., 2020; Yin & Struik, 2017). Therefore, many current models do not consider the drought acclimation of biochemical parameters. However, we found that both diffusional and biochemical parameters and their thermal sensitivity considerably acclimate to drought and the combination of drought and T_{growth}. Consequently, neglecting this acclimation would lead to critical errors in predicting leaf photosynthetic capacity, particularly under extreme conditions such as drought stress and heat shocks (i.e. when T_{leaf} is high). We have also shown that these acclimation responses to drought and T_{growth} cannot be explained by the altered leaf N content. Several alternative mechanisms have been discussed. Further research is needed to reveal mechanisms underlying these acclimation responses. In addition, the 'deacclimation' of photosynthesis related processes after rewatering should also be analysed. Finally, the priming effect of mild water deficit that may help plants cope with later and more severe drought (e.g. Wang et al., 2015) should also be considered. All these would provide empirical data that help develop

mechanistic algorithms for the photosynthetic acclimation to a set of environmental combinations across species, thereby minimizing uncertainties in global modelling framework for projecting the impact of climate change on (agro)ecosystems.

REFERENCES

Asseng, S., Ewert, F., Martre, P., Rötter, R. P., Lobell, D. B., Cammarano, D., Kimball, B. A., Ottman, M. J., Wall, G. W., White, J. W., Reynolds, M. P., Alderman, P. D., Prasad, P. V. V., Aggarwal, P. K., Anothai, J., Basso, B., Biernath, C., Challinor, A. J., De Sanctis, G., ... Zhu, Y. (2015). Rising temperatures reduce global wheat production. *Nature Climate Change*, 5(2), 143–147. https://doi.org/10.1038/nclimate2470

Barber, H. M., Carney, J., Alghabari, F., & Gooding, M. J. (2015). Decimal growth stages for precision wheat production in changing environments? *Annals of Applied Biology*, 166(3), 355–371. https://doi.org/10.1111/aab.12207

Bernacchi, C. J., Pimentel, C., & Long, S. P. (2003). *In vivo* temperature response functions of parameters required to model RuBP-limited photosynthesis. *Plant, Cell & Environment*, 26(9), 1419–1430. https://doi.org/10.1046/j.0016-8025.2003.01050.x

Bernacchi, C. J., Rosenthal, D. M., Pimentel, C., Long, S. P., & Farquhar, G. D. (2009). Modeling the temperature dependence of C_3 photosynthesis. In Laisk, A., Nedbal, L. & Govindjee (Eds.), *Photosynthesis in silico: Understanding complexity from molecules to ecosystems* (pp. 231–246). Springer. https://doi.org/10.1007/978-1-4020-9237-4_10

Cai, C., Li, G., Di, L., Ding, Y., Fu, L., Guo, X., Struik, P. C., Pan, G., Li, H., Chen, W., Luo, W., & Yin, X. (2020). The acclimation of leaf photosynthesis of wheat and rice to seasonal temperature changes in T-FACE environments. *Global Change Biology*, 26(2), 539–556. https://doi.org/10.1111/gcb.14830

Cai, C., Li, G., Yang, H., Yang, J., Liu, H., Struik, P. C., Luo, W., Yin, X., Di, L., Guo, X., Jiang, W., Si, C., Pan, G., & Zhu, J. (2018). Do all leaf photosynthesis parameters of rice acclimate to elevated CO_2, elevated temperature, and their combination, in FACE environments? *Global Change Biology*, 24(4), 1685–1707. https://doi.org/10.1111/gcb.13961

Campos, H., Trejo, C., Peña-Valdivia, C. B., García-Nava, R., Conde-Martínez, F. V., & Cruz-Ortega, M. R. (2014). Stomatal and non-stomatal limitations of bell pepper (*Capsicum annuum* L.) plants under water stress and re-watering: Delayed restoration of photosynthesis during recovery. *Environmental and Experimental Botany*, 98, 56–64. https://doi.org/10.1016/j.envexpbot.2013.10.015

Centritto, M., Lauteri, M., Monteverdi, M. C., & Serraj, R. (2009). Leaf gas exchange, carbon isotope discrimination, and grain yield in contrasting rice genotypes subjected to water deficits during the reproductive stage. *Journal of Experimental Botany*, 60(8), 2325–2339. https://doi.org/10.1093/jxb/erp123

Crous, K. Y., Drake, J. E., Aspinwall, M. J., Sharwood, R. E., Tjoelker, M. G., & Ghannoum, O. (2018). Photosynthetic capacity and leaf nitrogen decline along a controlled climate gradient in provenances of two widely distributed eucalyptus species. *Global Change Biology*, 24(10), 4626–4644. https://doi.org/10.1111/gcb.14330

Dai, L., Xu, Y., Harmens, H., Duan, H., Feng, Z., Hayes, F., Sharps, K., Radbourne, A., & Tarvainen, L. (2021). Reduced photosynthetic thermal acclimation capacity under elevated ozone in poplar (*Populus tremula*) saplings. *Global Change Biology*, 27(10), 2159–2173. https://doi.org/10.1111/gcb.15564

Dusenge, M. E., Madhavji, S., & Way, D. A. (2020). Contrasting acclimation responses to elevated CO_2 and warming between an evergreen and a deciduous boreal conifer. *Global Change Biology*, 26(6), 3639–3657. https://doi.org/10.1111/gcb.15084

Dusenge, M. E., Wittemann, M., Mujawamariya, M., Ntawuhiganayo, E. B., Zibera, E., Ntirugulirwa, B., Way, D. A., Nsabimana, D., Uddling, J., & Wallin, G. (2021). Limited thermal acclimation of photosynthesis in tropical montane tree species. *Global Change Biology*, 27(19), 4860–4878. https://doi.org/10.1111/gcb.15790

Fang, L., Yin, X., van der Putten, P. E., Martre, P., & Struik, P. C. (2022). Drought exerts a greater influence than growth temperature on the temperature response of leaf day respiration in wheat (*Triticum aestivum*). *Plant, Cell & Environment*, 45(7), 2062–2077. https://doi.org/10.1111/pce.14324

Farquhar, G. D., von Caemmerer, S. V., & Berry, J. A. (1980). A biochemical model of photosynthetic CO_2 assimilation in leaves of C_3 species. *Planta*, 149(1), 78–90. https://doi.org/10.1007/BF00386231

Flexas, J., & Diaz-Espejo, A. (2015). Interspecific differences in temperature response of mesophyll conductance: Food for thought on its origin and regulation. *Plant, Cell & Environment*, 38(4), 625–628. https://doi.org/10.1111/pce.12476

Flexas, J., Diaz-Espejo, A., Galmes, J., Kaldenhoff, R., Medrano, H., & Ribas-Carbó, M. (2007). Rapid variations of mesophyll conductance in response to changes in CO_2 concentration around leaves. *Plant, Cell & Environment*, 30(10), 1284–1298. https://doi.org/10.1111/j.1365-3040.2007.01700.x

Flexas, J., & Medrano, H. (2002). Drought-inhibition of photosynthesis in C_3 plants: Stomatal and non-stomatal limitations revisited. *Annals of Botany*, 89(2), 183–189. https://doi.org/10.1093/aob/mcf027

Galmés, J., Aranjuelo, I., Medrano, H., & Flexas, J. (2013). Variation in rubisco content and activity under variable climatic factors. *Photosynthesis Research*, *117*(1), 73–90. https://doi.org/10.1007/s11120-013-9861-y

Galmés, J., Kapralov, M. V., Copolovici, L. O., Hermida-Carrera, C., & Niinemets, Ü. (2015). Temperature responses of the rubisco maximum carboxylase activity across domains of life: Phylogenetic signals, trade-offs, and importance for carbon gain. *Photosynthesis Research*, *123*(2), 183–201. https://doi.org/10.1007/s11120-014-0067-8

Galmés, J., Ribas-Carbó, M., Medrano, H., & Flexas, J. (2011). Rubisco activity in Mediterranean species is regulated by the chloroplastic CO_2 concentration under water stress. *Journal of Experimental Botany*, *62*(2), 653–665. https://doi.org/10.1093/jxb/erq303

Genty, B., Briantais, J. M., & Baker, N. R. (1989). The relationship between the quantum yield of photosynthetic electron transport and quenching of chlorophyll fluorescence. *Biochimica et Biophysica Acta (BBA)-General Subjects*, *990*(1), 87–92. https://doi.org/10.1016/S0304-4165(89)80016-9

Girousse, C., Inchboard, L., Deswarte, J. C., & Chenu, K. (2021). How does post-flowering heat impact grain growth and its determining processes in wheat? *Journal of Experimental Botany*, *72*(18), 6596–6610. https://doi.org/10.1093/jxb/erab282

Gu, J., Yin, X., Stomph, T., & Struik, P. C. (2014). Can exploiting natural genetic variation in leaf photosynthesis contribute to increasing rice productivity? A simulation analysis. *Plant, Cell & Environment*, *37*(1), 22–34. https://doi.org/10.1111/pce.12173

Harbinson, J., & Yin, X. (2022). Modelling the impact of improved photosynthetic properties on crop performance in Europe. *Food and Energy Security*. https://doi.org/10.1002/fes3.402 (in press).

Harley, P. C., & Sharkey, T. D. (1991). An improved model of C_3 photosynthesis at high CO_2: Reversed O_2 sensitivity explained by lack of glycerate reentry into the chloroplast. *Photosynthesis Research*, *27*(3), 169–178. https://doi.org/10.1007/BF00035838

Harley, P. C., Thomas, R. B., Reynolds, J. F., & Strain, B. R. (1992). Modelling photosynthesis of cotton grown in elevated CO_2. *Plant, Cell & Environment*, *15*(3), 271–282. https://doi.org/10.1111/j.1365-3040.1992.tb00974.x

Hikosaka, K., Ishikawa, K., Borjigidai, A., Muller, O., & Onoda, Y. (2006). Temperature acclimation of photosynthesis: Mechanisms involved in the changes in temperature dependence of photosynthetic rate. *Journal of Experimental Botany*, *57*(2), 291–302. https://doi.org/10.1093/jxb/erj049

Huang, M., Piao, S., Ciais, P., Peñuelas, J., Wang, X., Keenan, T. F., Peng, S., Berry, J. A., Wang, K., Mao, J., Alkama, R., Cescatti, A., Cuntz, M., De Deurwaerder, H., Gao, M., He, Y., Liu, Y., Luo, Y., Myneni, R. B., … Janssens, I. A. (2019). Air temperature optima of vegetation productivity across global biomes. *Nature Ecology & Evolution*, *3*(5), 772–779. https://doi.org/10.1038/s41559-019-0838-x

IPCC. (2021). Climate change 2021: The physical science basis. In V. Masson-Delmotte, P. Zhai, & A. Pirani (Eds.), *Contribution of working group I to the sixth assessment report of the intergovernmental panel on climate change* (2391 pp). Cambridge University Press. https://doi.org/10.1017/9781009157896

June, T., Evans, J. R., & Farquhar, G. D. (2004). A simple new equation for the reversible temperature dependence of photosynthetic electron transport: A study on soybean leaf. *Functional Plant Biology*, *31*(3), 275–283. https://doi.org/10.1071/FP03250

Kattge, J., & Knorr, W. (2007). Temperature acclimation in a biochemical model of photosynthesis: A reanalysis of data from 36 species. *Plant, Cell & Environment*, *30*(9), 1176–1190. https://doi.org/10.1111/j.1365-3040.2007.01690.x

Kumarathunge, D. P., Drake, J. E., Tjoelker, M. G., López, R., Pfautsch, S., Vårhammar, A., & Medlyn, B. E. (2020). The temperature optima for tree seedling photosynthesis and growth depend on water inputs.

Global Change Biology, *26*(4), 2544–2560. https://doi.org/10.1111/gcb.14975

Kumarathunge, D. P., Medlyn, B. E., Drake, J. E., Tjoelker, M. G., Aspinwall, M. J., Battaglia, M., Cano, F. J., Carter, K. R., Cavaleri, M. A., Cernusak, L. A., Chambers, J. Q., Crous, K. Y., De Kauwe, M. G., Dillaway, D. N., Dreyer, E., Ellsworth, D. S., Ghannoum, O., Han, Q., Hikosaka, K., … Way, D. A. (2019). Acclimation and adaptation components of the temperature dependence of plant photosynthesis at the global scale. *New Phytologist*, *222*(2), 768–784. https://doi.org/10.1111/nph.15668

Leuning, R. (2002). Temperature dependence of two parameters in a photosynthesis model. *Plant, Cell & Environment*, *25*(9), 1205–1210. https://doi.org/10.1046/j.1365-3040.2002.00898.x

Lloret, F., Escudero, A., Iriondo, J. M., Martínez-Vilalta, J., & Valladares, F. (2012). Extreme climatic events and vegetation: The role of stabilizing processes. *Global Change Biology*, *18*(3), 797–805. https://doi.org/10.1111/j.1365-2486.2011.02624.x

Lobell, D. B., & Gourdji, S. M. (2012). The influence of climate change on global crop productivity. *Plant Physiology*, *160*(4), 1686–1697. https://doi.org/10.1104/pp.112.208298

Loriaux, S. D., Avenson, T. J., Welles, J. M., McDermitt, D. K., Eckles, R. D., Riensche, B., & Genty, B. (2013). Closing in on maximum yield of chlorophyll fluorescence using a single multiphase flash of subsaturating intensity. *Plant, Cell & Environment*, *36*(10), 1755–1770. https://doi.org/10.1111/pce.12115

Lu, C., & Zhang, J. (1999). Effects of water stress on photosystem II photochemistry and its thermostability in wheat plants. *Journal of Experimental Botany*, *50*(336), 1199–1206. https://doi.org/10.1093/jxb/50.336.1199

Ma, W. T., Tcherkez, G., Wang, X. M., Schäufele, R., Schnyder, H., Yang, Y., & Gong, X. Y. (2021). Accounting for mesophyll conductance substantially improves ^{13}C-based estimates of intrinsic water-use efficiency. *New Phytologist*, *229*(3), 1326–1338. https://doi.org/10.1111/nph.16958

Martre, P., Porter, J. R., Jamieson, P. D., & Triboï, E. (2003). Modeling grain nitrogen accumulation and protein composition to understand the sink/source regulations of nitrogen remobilization for wheat. *Plant Physiology*, *133*(4), 1959–1967. https://doi.org/10.1104/pp.103.030585

Medlyn, B. E., Dreyer, E., Ellsworth, D., Forstreuter, M., Harley, P. C., Kirschbaum, M. U. F., Le Roux, X., Montpied, P., Strassemeyer, J., Walcroft, A., Wang, K., & Loustau, D. (2002). Temperature response of parameters of a biochemically based model of photosynthesis. II. A review of experimental data. *Plant, Cell & Environment*, *25*(9), 1167–1179. https://doi.org/10.1046/j.1365-3040.2002.00891.x

Mercado, L. M., Medlyn, B. E., Huntingford, C., Oliver, R. J., Clark, D. B., Sitch, S., Zelazowski, P., Kattge, J., Harper, A. B., & Cox, P. M. (2018). Large sensitivity in land carbon storage due to geographical and temporal variation in the thermal response of photosynthetic capacity. *New Phytologist*, *218*(4), 1462–1477. https://doi.org/10.1111/nph.15100

Moore, C. E., Meacham-Hensold, K., Lemonnier, P., Slattery, R. A., Benjamin, C., Bernacchi, C. J., Lawson, T., & Cavanagh, A. P. (2021). The effect of increasing temperature on crop photosynthesis: From enzymes to ecosystems. *Journal of Experimental Botany*, *72*(8), 2822–2844. https://doi.org/10.1093/jxb/erab090

Ouyang, W., Struik, P. C., Yin, X., & Yang, J. (2017). Stomatal conductance, mesophyll conductance, and transpiration efficiency in relation to leaf anatomy in rice and wheat genotypes under drought. *Journal of Experimental Botany*, *68*(18), 5191–5205. https://doi.org/10.1093/jxb/erx314

Peng, B., Guan, K., Tang, J., Ainsworth, E. A., Asseng, S., Bernacchi, C. J., Cooper, M., Delucia, E. H., Elliott, J. W., Ewert, F., Grant, R. F., Gustafson, D. I., Hammer, G. L., Jin, Z., Jones, J. W., Kimm, H., Lawrence, D. M., Li, Y., Lombardozzi, D. L., … Zhou, W. (2020).

Towards a multiscale crop modelling framework for climate change adaptation assessment. *Nature Plants*, 6(4), 338–348. https://doi.org/10.1038/s41477-020-0625-3

Perdomo, J. A., Capó-Bauçà, S., Carmo-Silva, E., & Galmés, J. (2017). Rubisco and rubisco activase play an important role in the biochemical limitations of photosynthesis in rice, wheat, and maize under high temperature and water deficit. *Frontiers in Plant Science*, 8, 490. https://doi.org/10.3389/fpls.2017.00490

Perkins-Kirkpatrick, S. E., & Lewis, S. C. (2020). Increasing trends in regional heatwaves. *Nature Communications*, 11(1), 1–8. https://doi.org/10.1038/s41467-020-16970-7

Piao, S., Sitch, S., Ciais, P., Friedlingstein, P., Peylin, P., Wang, X., Ahlström, A., Anav, A., Canadell, J. G., Cong, N., Huntingford, C., Jung, M., Levis, S., Levy, P. E., Li, J., Lin, X., Lomas, M. R., Lu, M., Luo, Y., … Zeng, N. (2013). Evaluation of terrestrial carbon cycle models for their response to climate variability and to CO_2 trends. *Global Change Biology*, 19(7), 2117–2132. https://doi.org/10.1111/gcb.12187

Posch, B. C., Kariyawasam, B. C., Bramley, H., Coast, O., Richards, R. A., Reynolds, M. P., Trethowan, R., & Atkin, O. K. (2019). Exploring high temperature responses of photosynthesis and respiration to improve heat tolerance in wheat. *Journal of Experimental Botany*, 70(19), 5051–5069. https://doi.org/10.1093/jxb/erz257

Rogers, A., Kumarathunge, D. P., Lombardozzi, D. L., Medlyn, B. E., Serbin, S. P., & Walker, A. P. (2020). Triose phosphate utilization limitation: An unnecessary complexity in terrestrial biosphere model representation of photosynthesis. *New Phytologist*, 230(1), 17–22. https://doi.org/10.1111/nph.17092

Salvucci, M. E., & Crafts-Brandner, S. J. (2004). Inhibition of photosynthesis by heat stress: The activation state of rubisco as a limiting factor in photosynthesis. *Physiologia Plantarum*, 120(2), 179–186. https://doi.org/10.1111/j.0031-9317.2004.0173.x

Sharkey, T. D. (1985). Photosynthesis in intact leaves of C_3 plants: Physics, physiology and rate limitations. *The Botanical Review*, 51(1), 53–105. https://doi.org/10.1007/BF02861058

Slot, M., Garcia, M. N., & Winter, K. (2016). Temperature response of CO_2 exchange in three tropical tree species. *Functional Plant Biology*, 43(5), 468–478. https://doi.org/10.1071/FP15320

Smith, N. G., & Dukes, J. S. (2013). Plant respiration and photosynthesis in global-scale models: Incorporating acclimation to temperature and CO_2. *Global Change Biology*, 19(1), 45–63. https://doi.org/10.1111/j.1365-2486.2012.02797.x

Smith, N. G., Malyshev, S. L., Shevliakova, E., Kattge, J., & Dukes, J. S. (2016). Foliar temperature acclimation reduces simulated carbon sensitivity to climate. *Nature Climate Change*, 6(4), 407–411. https://doi.org/10.1038/nclimate2878

Solomon, S., Plattner, G. K., Knutti, R., & Friedlingstein, P. (2009). Irreversible climate change due to carbon dioxide emissions. *Proceedings of the National Academy of Sciences*, 106(6), 1704–1709. https://doi.org/10.1073/pnas.081272110

Tezara, W. M. V. J., Mitchell, V. J., Driscoll, S. D., & Lawlor, D. W. (1999). Water stress inhibits plant photosynthesis by decreasing coupling factor and ATP. *Nature*, 401(6756), 914–917. https://doi.org/10.1038/44842

von Caemmerer, S., & Evans, J. R. (2015). Temperature responses of mesophyll conductance differ greatly between species. *Plant, Cell & Environment*, 38(4), 629–637. https://doi.org/10.1111/pce.12449

von Caemmerer, S., Farquhar, G., & Berry, J. (2009). Biochemical model of C_3 photosynthesis. In Laisk, A., Nedbal, L. & Govindjee (Eds.), *Photosynthesis in silico: Understanding complexity from molecules to ecosystems* (pp. 209–230). Springer. https://doi.org/10.1007/978-1-4020-9237-4_9

Wang, D., Rianti, W., Gálvez, F., van der Putten, P. E., Struik, P. C., & Yin, X. (2022). Estimating photosynthetic parameter values of rice, wheat, maize and sorghum to enable smart crop cultivation. *Crop and Environment*, 1(2), 119–132. https://doi.org/10.1016/j.crope.2022.05.004

Wang, X., Vignjevic, M., Liu, F., Jacobsen, S., Jiang, D., & Wollenweber, B. (2015). Drought priming at vegetative growth stages improves tolerance to drought and heat stresses occurring during grain filling in spring wheat. *Plant Growth Regulation*, 75(3), 677–687. https://doi.org/10.1007/s10725-014-9969-x

Warren, C. R. (2008). Stand aside stomata, another actor deserves Centre stage: The forgotten role of the internal conductance to CO_2 transfer. *Journal of Experimental Botany*, 59(7), 1475–1487. https://doi.org/10.1093/jxb/erm245

Way, D. A., & Yamori, W. (2014). Thermal acclimation of photosynthesis: On the importance of adjusting our definitions and accounting for thermal acclimation of respiration. *Photosynthesis Research*, 119(1), 89–100. https://doi.org/10.1007/s11120-013-9873-7

Wei, Z., Fang, L., Li, X., Liu, J., & Liu, F. (2020). Effects of elevated atmospheric CO_2 on leaf gas exchange response to progressive drought in barley and tomato plants with different endogenous ABA levels. *Plant and Soil*, 447(1), 431–446. https://doi.org/10.1007/s11104-019-04393-3

Yamasaki, T., Yamakawa, T., Yamane, Y., Koike, H., Satoh, K., & Katoh, S. (2002). Temperature acclimation of photosynthesis and related changes in photosystem II electron transport in winter wheat. *Plant Physiology*, 128(3), 1087–1097. https://doi.org/10.1104/pp.010919

Yamori, W., Hikosaka, K., & Way, D. A. (2014). Temperature response of photosynthesis in C_3, C_4, and CAM plants: Temperature acclimation and temperature adaptation. *Photosynthesis Research*, 119(1), 101–117. https://doi.org/10.1007/s11120-013-9874-6

Yamori, W., Noguchi, K., Hanba, Y. T., & Terashima, I. (2006). Effects of internal conductance on the temperature dependence of the photosynthetic rate in spinach leaves from contrasting growth temperatures. *Plant and Cell Physiology*, 47(8), 1069–1080. https://doi.org/10.1093/pcp/pcj077

Yamori, W., Noguchi, K. O., & Terashima, I. (2005). Temperature acclimation of photosynthesis in spinach leaves: Analyses of photosynthetic components and temperature dependencies of photosynthetic partial reactions. *Plant, Cell & Environment*, 28(4), 536–547. https://doi.org/10.1111/j.1365-3040.2004.01299.x

Yang, J. T., Preiser, A. L., Li, Z., Weise, S. E., & Sharkey, T. D. (2016). Triose phosphate use limitation of photosynthesis: Short-term and long-term effects. *Planta*, 243(3), 687–698. https://doi.org/10.1007/s00425-015-2436-8

Yin, X. (2013). Improving ecophysiological simulation models to predict the impact of elevated atmospheric CO_2 concentration on crop productivity. *Annals of Botany*, 112(3), 465–475. https://doi.org/10.1093/aob/mct016

Yin, X. (2021). No need to switch the modified Arrhenius function back to the old form. *New Phytologist*, 231(6), 2113–2116. https://doi.org/10.1111/nph.17341

Yin, X., Belay, D. W., van der Putten, P. E., & Struik, P. C. (2014). Accounting for the decrease of photosystem photochemical efficiency with increasing irradiance to estimate quantum yield of leaf photosynthesis. *Photosynthesis Research*, 122(3), 323–335. https://doi.org/10.1007/s11120-014-0030-8

Yin, X., Gu, J., Dingkuhn, M., & Struik, P. C. (2022). A model-guided holistic review of exploiting natural variation of photosynthesis traits in crop improvement. *Journal of Experimental Botany*, 73(10), 3173–3188. https://doi.org/10.1093/jxb/erac109

Yin, X., Schapendonk, A. H., & Struik, P. C. (2019). Exploring the optimum nitrogen partitioning to predict the acclimation of C_3 leaf photosynthesis to varying growth conditions. *Journal of Experimental Botany*, 70(9), 2435–2447. https://doi.org/10.1093/jxb/ery277

Yin, X., & Struik, P. C. (2009). Theoretical reconsiderations when estimating the mesophyll conductance to CO_2 diffusion in leaves of C_3 plants by analysis of combined gas exchange and chlorophyll fluorescence measurements. *Plant, Cell & Environment*, 32(11), 1513–1524. https://doi.org/10.1111/j.1365-3040.2009.02016.x

Yin, X., & Struik, P. C. (2017). Can increased leaf photosynthesis be converted into higher crop mass production? A simulation study for rice using the crop model GECROS. *Journal of Experimental Botany*, *68*(9), 2345–2360. https://doi.org/10.1093/jxb/erx085

Yin, X., Struik, P. C., Romero, P., Harbinson, J., Evers, J. B., Van Der Putten, P. E., & Vos, J. A. N. (2009). Using combined measurements of gas exchange and chlorophyll fluorescence to estimate parameters of a biochemical C$_3$ photosynthesis model: A critical appraisal and a new integrated approach applied to leaves in a wheat (*Triticum aestivum*) canopy. *Plant, Cell & Environment*, *32*(5), 448–464. https://doi.org/10.1111/j.1365-3040.2009.01934.x

Yin, X., Van Der Putten, P. E., Driever, S. M., & Struik, P. C. (2016). Temperature response of bundle-sheath conductance in maize leaves. *Journal of Experimental Botany*, *67*(9), 2699–2714. https://doi.org/10.1093/jxb/erw104

Yin, X., & van Laar, H. H. (2005). *Crop systems dynamics: An ecophysiological simulation model of genotype-by-environment interactions.* Wageningen Academic Publishers. https://edepot.wur.nl/139772

Zivcak, M., Brestic, M., Balatova, Z., Drevenakova, P., Olsovska, K., Kalaji, H. M., Yang, X., & Allakhverdiev, S. I. (2013). Photosynthetic electron transport and specific photoprotective responses in wheat leaves under drought stress. *Photosynthesis Research*, *117*(1), 529–546. https://doi.org/10.1007/s11120-013-9885-3

SUPPORTING INFORMATION

Additional supporting information can be found online in the Supporting Information section at the end of this article.